A Quantitative Evaluation of the AVITEWRITE Model of Handwriting Learning

R. W. Paine *, S. Grossberg **, A. W. A. Van Gemmert ***

* RIKEN Brain Science Institute, Laboratory for Behavior and Dynamic Cognition, 2-1 Hirosawa, Wako-shi, Saitama 351-0198, Japan; ** Boston University, Department of Cognitive and Neural Systems, 677 Beacon St., Boston, MA 02215; *** Arizona State University, Department of Kinesiology, Motor Control Laboratory, PO Box 870404, Tempe, AZ 85287-0404

Human Movement Science, in press.

* R.W. Paine was supported in part by DARPA/ONR N00014-95-1-0409, NIH 1 R29-DC02952-01, and ONR N00014-92-J-1309.

** S. Grossberg was supported in part by AFOSR F49620-01-1-0397 and ONR N00014-01-1-0624.

*** A. W. A. Van Gemmert was supported in part by NINDS NS 33173.

Abstract

Much sensory-motor behavior develops through imitation, as during the learning of handwriting by children. Such complex sequential acts are broken down into distinct motor control synergies, or muscle groups, whose activities overlap in time to generate continuous, curved movements that obey an inverse relation between curvature and speed. The Adaptive Vector Integration to Endpoint Handwriting (AVITEWRITE) model of Grossberg and Paine (2000) addressed how such complex movements may be learned through attentive imitation. The model suggested how parietal and motor cortical mechanisms, such as difference vector encoding, interact with adaptively-timed, predictive cerebellar learning during movement imitation and predictive performance. Key psychophysical and neural data about learning to make curved movements were simulated, including a decrease in writing time as learning progresses; generation of unimodal, bell-shaped velocity profiles for each movement synergy; size scaling with isochrony, and speed scaling with preservation of the letter shape and the shapes of the velocity profiles; an inverse relation between curvature and tangential velocity; and a Two-Thirds Power Law relation between angular velocity and curvature. However, the model learned from letter trajectories of only one subject, and only qualitative kinematic comparisons were made with previously published human data. The present work describes a quantitative test of AVITEWRITE through direct comparison of a corpus of human handwriting data with the model's performance when it learns by tracing the human trajectories. The results show that model performance was variable across the subjects, with an average correlation between the model and human data of 0.89 +/-0.10. The present data from simulations using the AVITEWRITE model highlight some of its strengths while focusing attention on areas, such as novel shape learning in children, where all models of handwriting and the learning of other complex sensory-motor skills would benefit from further research.

I. INTRODUCTION

How do children learn curvilinear movements by imitating written letters? How do varying, error-prone movements during learning become correct, efficient movements after repeated trials? The Adaptive VITEWRITE (AVITEWRITE) model of Grossberg and Paine (2000) attempts to answer these questions by modeling the perception/action cycle of handwriting. Although Grossberg and Paine (2000) demonstrated good qualitative performance of AVITEWRITE, the model learned from letter trajectories of only one subject, and only qualitative kinematic comparisons were made with previously published human data. Since a model may yield good qualitative performance, yet still be unable to capture the details and variability of human performance, a quantitative test of AVITEWRITE is conducted here, clarifying its strengths and weaknesses through direct comparison with a corpus of human handwriting data.

AVITEWRITE describes how the complex sequences of movements involved in handwriting can be learned through the imitation of previously drawn curves. The model shows how initially segmented movements with multimodal velocity profiles during the early stages of learning, corresponding to early childhood, can become the smooth, continuous movements with the unimodal, bell-shaped velocity profiles observed in adult humans (Abend et al., 1982; Edelman & Flash, 1987; Morasso, 1981; Morasso et al., 1983) after multiple learning trials. Early, error-prone handwriting movements with many visually reactive, correctional components gradually improve over time and many learning trials, to become automatic, error-free movements. These movements can even be performed without visual feedback, as when a human signs his name with his eyes shut.

The AVITEWRITE model architecture is schematized in Fig. 1. The model attempts to explain aspects of how visually reactive and planned movement commands can cooperate or compete to determine what movement will next occur. Because the planned commands are typically learned, the model proposes how new learning can occur even during reactive movements before becoming the basis for later planned movements that are read out of memory. At the start of movement, visual attention (1) focuses on the current hand position and moves to select a target position (2) on the curve being traced. A Difference Vector representation (3) of the distance and direction to the target is formed between an efference copy of the current hand position (*PPV*) and the new target position (*TPV*) (Andersen, 1995; Bullock, Cisek & Grossberg, 1998; Bullock & Grossberg, 1988; Georgopoulos et al., 1982; Mussa-Ivaldi, 1988). This Difference Vector activates the appropriate muscle synergy (4) to drive a reactive movement to that target. At the same time, a cerebellar adaptive timing system (5) learns the activation pattern of the muscle synergy involved in the movement.

Adaptive timing of strokes may be achieved by spectral timing in the cerebellum. Fiala et al. (1996) and others (Ito, 1984; Perrett, Ruiz, & Mauk, 1993) suggest that the cerebellum may be involved in the opening of a timed gate to express a learned motor gain. A Conditioned Stimulus arrives via parallel fibers at a population of cerebellar Purkinje cells, triggering a spectrum of phase-delayed depolarizations of the Purkinje cells. When a teaching signal is triggered by an Unconditioned Stimulus in climbing fibers at some fixed Interstimulus Interval after the Conditioned Stimulus, then Long Term Depression of the Purkinje cells may occur at that time, leading to disinhibition of

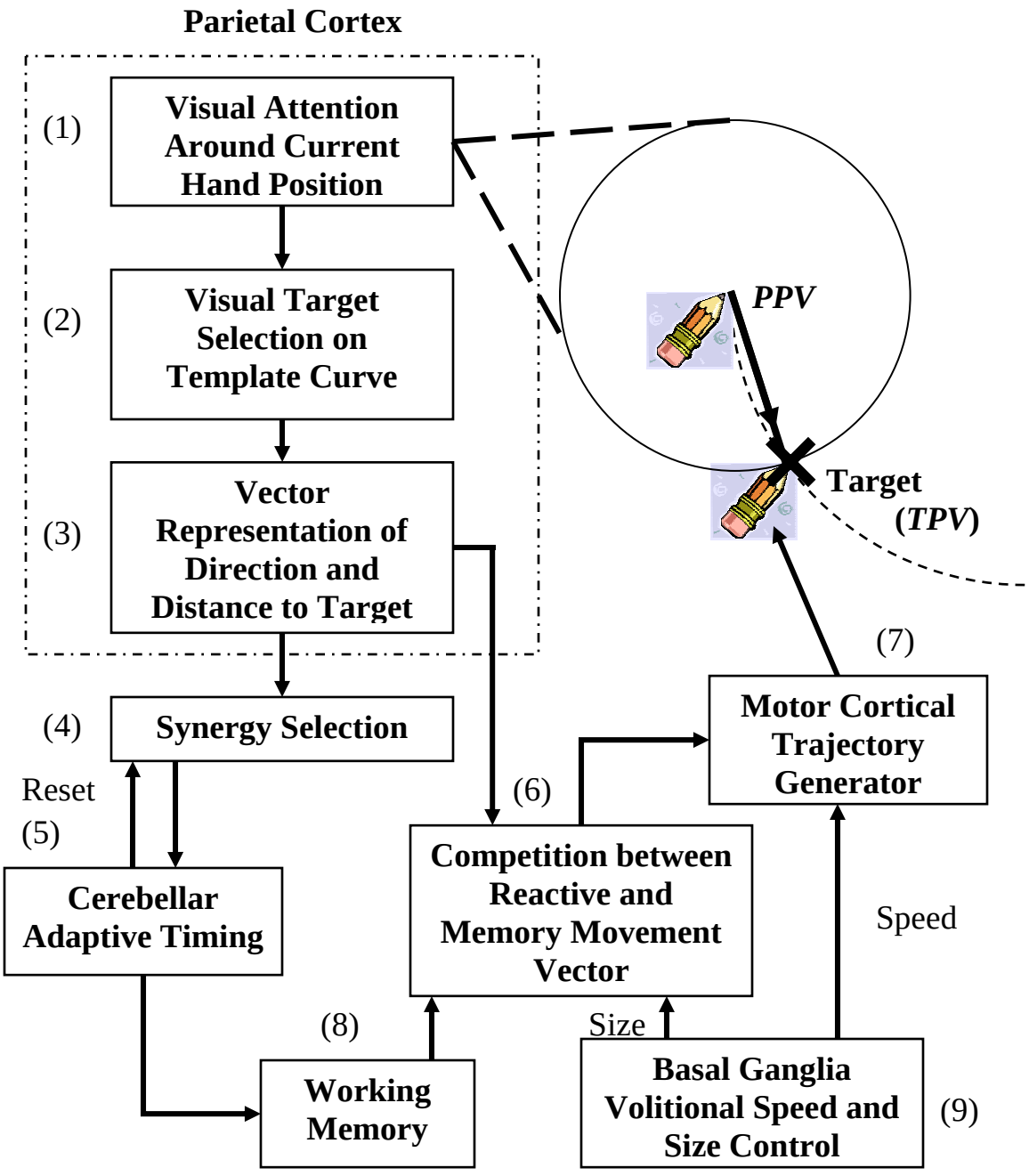

Fig. 1. Conceptual diagram of the AVITEWRITE architecture. Numbers in parentheses indicate the order of discussion in the text. *PPV*: Present Position Vector; *TPV*: Target Position Vector.

the cerebellar nuclei at that time; hence the term "adaptive timing" (Fiala, Grossberg, & Bullock, 1996; Grossberg & Merrill, 1992, 1996).

The cerebellar adaptive timing system begins to cooperate or compete (6) with reactive visual attention for control of the motor cortical trajectory generator (7). A working memory (8) transiently stores learned motor commands to allow them to be

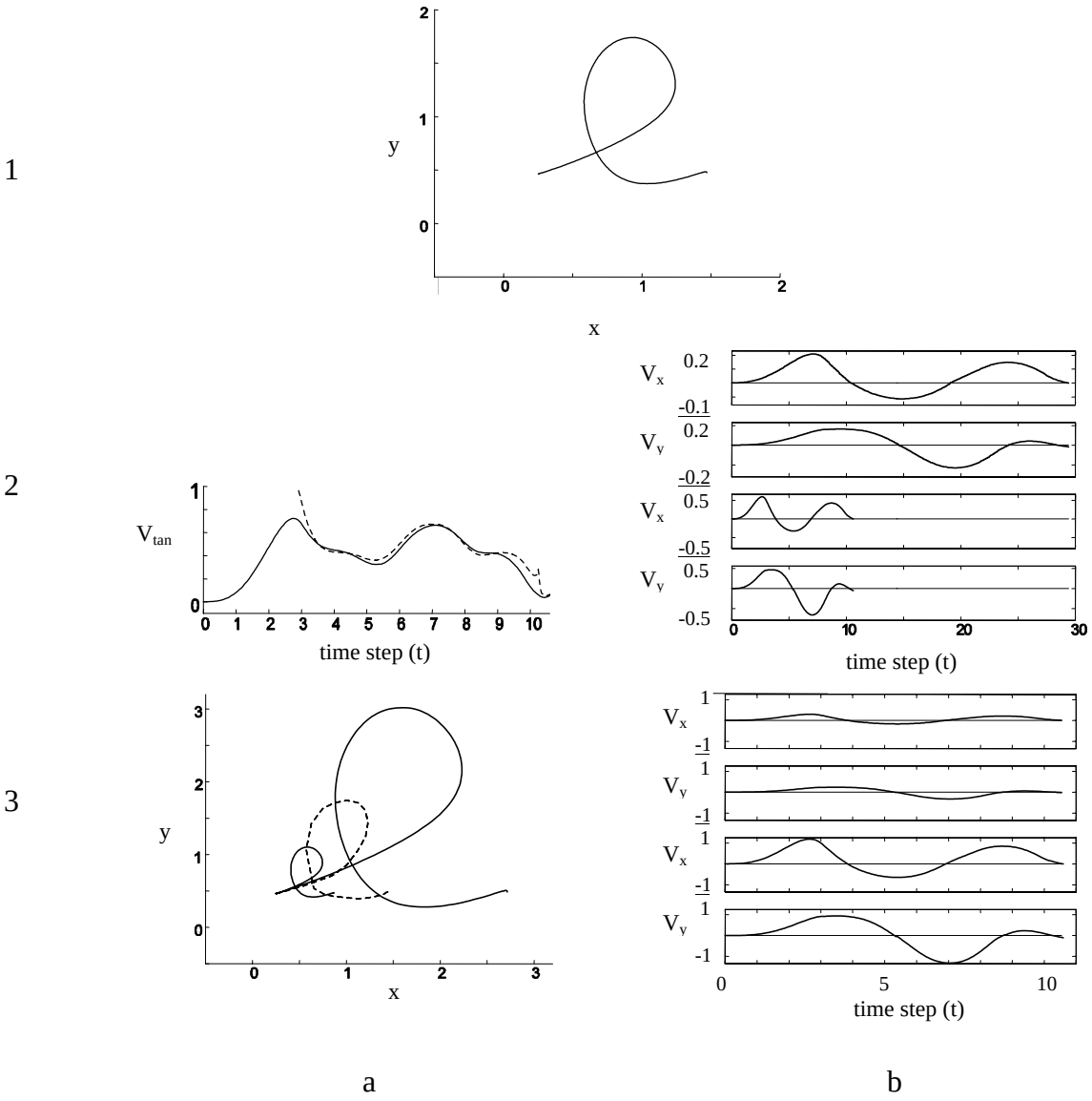

Fig. 2. Example of AVITEWRITE's writing and various psychophysical properties: (1) Letter *L* learned by tracing a human trajectory; (2a) Tangential velocity of the model's letter *L* (solid) compared to that predicted by the 2/3 power law (dash); (2b) Velocity profiles after scaling the writing speed of the letter *L* with trajectory invariance; (3a) Size scaling of the letter *L*, halving and doubling the original (dash); (3b) Velocity profiles after size scaling, exhibiting isochrony. Reproduced with permission from Grossberg & Paine (2000).

executed at decreased speeds as the speed and size of trajectory generation are volitionally controlled through the basal ganglia (9). Reactive visual control takes over when planned read-out from memory causes mistakes, defined as deviation beyond the attention radius around the curve. Both the movement trajectory and the memory are then corrected, allowing memory to take over control again. As successive, visually reactive

movements are made to a series of attentionally chosen targets on the curve, a memory is formed of the muscle synergy activations needed to draw that curve. After tracing the curve multiple times, planned read-out from memory alone can yield error-free movements.

Several properties of human handwriting movements emerge when AVITEWRITE learns to write a letter (Fig. 2). Size and speed can be volitionally varied (Fig. 1, stage 9) after learning while preserving letter shape and the shapes of the velocity profiles (Plamondon et al. 1997; Schillings et al., 1996; van Galen & Weber, 1998; Wann & Nimmo-Smith, 1990; Wright, 1993). Isochrony, the tendency for humans to write letters of different sizes in the same amount of time, is also an emergent property of model interactions (Thomassen & Teulings, 1985; Wright, 1993; Van Gemmert, Adler, & Stelmach, 2003). Speed can be varied during learning, and learning at slower speeds facilitates future learning at faster speeds (Alston & Taylor, 1987, p. 115; Burns, 1962, pp. 45-46; Freeman, 1914, pp. 83-84). Unimodal, bell-shaped velocity profiles for each movement synergy emerge as a letter is learned, and they closely resemble the velocity profiles of adult humans writing those letters (Abend et al., 1982; Edelman & Flash, 1987; Morasso, 1981; Morasso et al., 1983). An inverse relation between curvature and tangential velocity is observed in the model's performance (Lacquaniti et al., 1983). It also yields a Two-Thirds Power Law relation between angular velocity and curvature, as seen in human writing under certain conditions (Lacquaniti et al., 1983; Thomassen & Teulings, 1985; Wann et al., 1988). Finally, context effects become apparent when AVITEWRITE generates multiple connected letters, reminiscent of carryover coarticulation in speech (Hertrich & Ackermann, 1995; Ostry et al., 1996), and are similar to handwriting context effects reported by Greer and Green (1983) and Thomassen and Schomaker (1986).

II. Methods

Handwriting data were collected from seven adult subjects. The subjects were asked to write separate strings of the letters e, l, i, o, and t (eeee..., llll..., etc.) using cursive handwriting on ten separate trials. Data were collected using a Wacom 12x18 Intuos digital writing tablet with an X and Y pen-tip position sampling frequency of 206 Hz. The raw position and time data were collected and velocity, acceleration, and curvature were calculated. The raw data were low pass filtered at 7Hz with a dual pass Butterworth fourth order digital filter to eliminate phase shift. The 7Hz cut-off frequency was selected to include all important writing frequency components, while reducing the effects of reflexes and other physiological tremor functions (Teulings & Maarse, 1984; Teulings & Stelmach, 1991; Van Gemmert, Adler, & Stelmach, 2003). The first letter of the string was selected as the single letter prototype for that subject's trial. Since the letters were connected, the vertical (y-direction) velocity zero crossings were used to determine strokes and separate adjacent letters. The rationale behind this is that cursive style letters are produced by a combination of up and down strokes and that letters are connected mainly by up strokes. Therefore, zero crossings in the vertical velocity do separate strokes and letters. The single-letter data from a subject's ten trials were averaged to create a letter prototype for that subject. Given that human movements are affected by modulation due to manipulation, impairment, or the natural variation inherent in biological systems, averaging is assumed to emphasize the invariant aspects of the

neural motor control program. In other words, it is believed to enhance the signal-to-noise ratio of the motor controller (Teulings & Stelmach, 1991). Nevertheless, one might argue that averaging distorts the letters to such a degree that individual letter styles are lost. To address this point, the averaged human data are compared to the unaveraged data for one subject. Specifically, the fifth trial of each letter was compared to the corresponding averaged letter for the subject. In order to examine the model's ability to capture any stylistic differences between the averaged and non-averaged data, AVITEWRITE was also trained using the same unaveraged human trials as input.

Each letter prototype was scaled in size (x and y range) for input to the AVITEWRITE model. A letter was matched in size to the corresponding letter learned in Grossberg and Paine (2000). Thus, the "L" of each subject was scaled to the same size for input into the model. Humans can immediately scale their writing size to a larger or smaller letter (Van Galen & Weber, 1998). This ability implies the use of an automatic size normalization process not present in the current model. Although AVITEWRITE can change writing size after learning, while preserving key features of the movement kinematics, it initially learns at the same size as its input since it uses a tracing strategy. For a given set of model parameters, using too small or too large an input trajectory during learning adversely affects learning convergence time and/or the generation of bell-shaped stroke velocity profiles.

AVITEWRITE learned to draw the letters after multiple learning trials, as described in Appendix Table 4. The end of a letter was defined as the falling of both x and y velocities below a threshold (0.006) when within a threshold distance of the end of the letter being traced. The letters learned by AVITEWRITE were then compared to the original human templates from which AVITEWRITE learned. Model performance was evaluated by calculating the correlations between the model trajectory, velocity, and acceleration with the human data. Model velocity and acceleration were first scaled to fit the time range and the maximal and minimal velocity and acceleration present in the corresponding human subject's data. Further, the correlation between the model's tangential velocity and the tangential velocity predicted by the two-thirds power law was calculated. The correlation between the human tangential velocity and that predicted by the two-thirds power law was also calculated. Correlations were calculated using Equation 14 in the Appendix, based on Equation 8 from Edelman and Flash (1987).

III. Results

The results of the simulations are shown in Figs. 3-6 for the best and worst model results on individual letters. The correlations between the model and the human data, averaged over x and y position, velocity, and acceleration over all letters for all subjects, are shown in Table 1. The correlations were calculated using Equation 14.

Note that some correlations exceed 1.0, as in the "1.04" correlation of y position in letter *i* of subject 1. This is an artifact of the correlation index used by Edelman and Flash (1987), who also reported correlations greater than 1.0 in some instances (c.f., their Figs. 3 to 6). Their equation is used here to allow direct comparison between their results and the present model. The results show that model performance was variable across the subjects, with a maximum total correlation of 1.0 and a minimum of 0.63. AVITEWRITE yields 0.89 +/- 0.10 mean correlation using a variable permissible time shift (r), and 0.80 +/- 0.12 using the more stringent requirement of 0 time shift between model and human

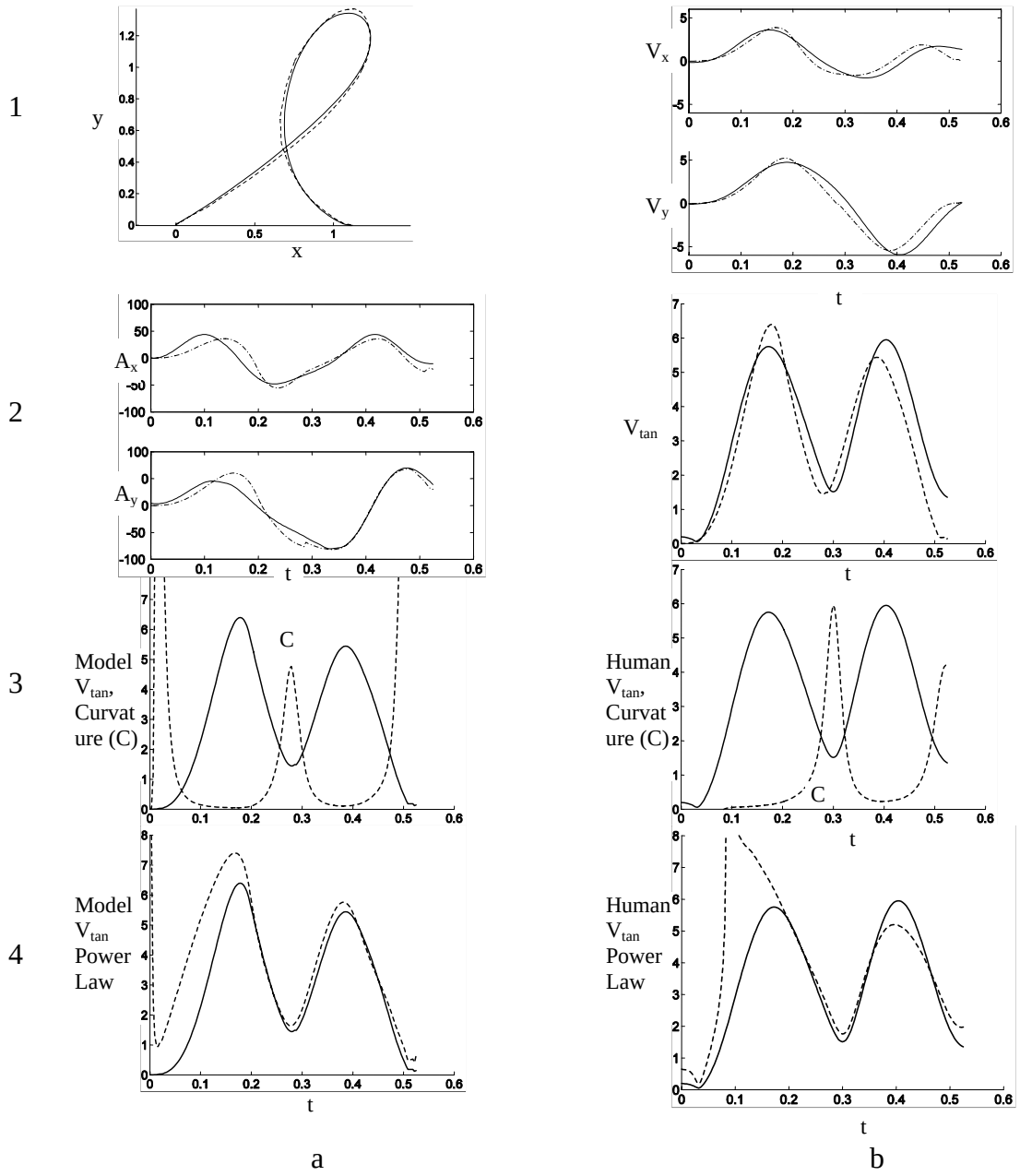

Fig. 3. Good correlations for *L* subject 1. (1a) Human (dash) and model (solid) trajectory; (1b) Human (solid) and model (dash) velocity (x top); (2a) Human (solid) and model (dash) acceleration (x top); (2b) Human (solid) and model (dash) tangential velocity; (3a) Model tangential velocity (solid) and curvature (dash); (3b) Human tangential velocity (solid) and curvature (dash); (4a) Model 2/3 power law tangential velocity prediction (dash) vs. actual model tangential velocity (solid); (4b) Human 2/3 power law tangential velocity prediction (dash) vs. actual human tangential velocity (solid).

Condition	Position	Velocity	Acceleration	Total
AVITEWRITE, r = variable, mean=5.2, range=[0:19]	0.96 +/- 0.06	0.83 +/- 0.14	0.77 +/- 0.20	0.89 +/- 0.10
AVITEWRITE, r = 0	0.92+/- 0.09	0.70 +/- 0.25	0.70 +/- 0.20	0.80 +/- 0.12
Minimum Snap, r = variable	0.98	0.99	0.97	0.97 +/- 0.003

Table 1. Overall Average Cross-Correlation with Standard Deviation between model and human data. *Top:* AVITEWRITE using variable correlation shift (r). *Middle:* AVITEWRITE using constant shift (r=0). *Bottom:* Minimum Snap Model of Edelman and Flash(1987) using variable shift (r).

Letter/ Subject	X Position	Y Position	Tangential Velocity	X Acceleration	Y Acceleration	Model 2/3 Power Law	Human 2/3 Power Law
E/1	0.89	1.03	0.86	0.95	1.03	0.85	0.77
L/1	0.98	0.99	0.95	0.91	0.97	0.95	0.89
I/1	0.98	1.04	0.90	0.90	1.02	0.56	0.85
O/7	1.01	1.01	0.96	0.93	0.96	0.98	0.89
T/4	1.00	1.00	0.87	0.82	0.84	0.81	0.89
E/2	0.95	0.91	0.70	0.45	0.29	0.74	0.86
L/2	0.98	0.93	0.59	0.67	0.30	0.79	0.85
I/5	0.82	0.93	0.36	0.37	0.46	0.65	0.74
O/3	0.73	0.82	0.86	0.37	0.43	0.86	0.91
T/3	0.94	1.00	0.47	0.89	0.96	0.88	0.93

Table 2. Correlations for Simulations Shown in Figs. 3-6: Best (top five rows) and Worst (bottom five rows) Results.

kinematic profiles (Table 1). Analysis of the worst-case simulation results (Figs. 4 and 6, Table 2), indicates that the main differences between the human data and model output are a variable stretching or compression of parts of the model velocity and acceleration profiles relative to the human profiles.

One should note that the available human data were not from individual letters, but from connected letters (eeee, llll, etc.). The first letter of each subject's sequence was selected for each of the ten trials per letter, after smoothing and averaging as described in the Methods. However, the human letter sequences did not generally have zero initial and final velocity and acceleration. In an attempt to collect handwriting samples in as natural a setting as possible, subjects were not specifically instructed to rest the pen at the starting position prior to beginning to write. As a result, their hands were already in motion when the pen contacted the writing surface. Hence, there is a problem with non-zero starting and stopping velocities in the human data against which the model was compared, in contrast with the zero velocity and acceleration initial conditions and equifinality observed in the AVITEWRITE model output, as seen in Figs. 3 and 4 (1b,

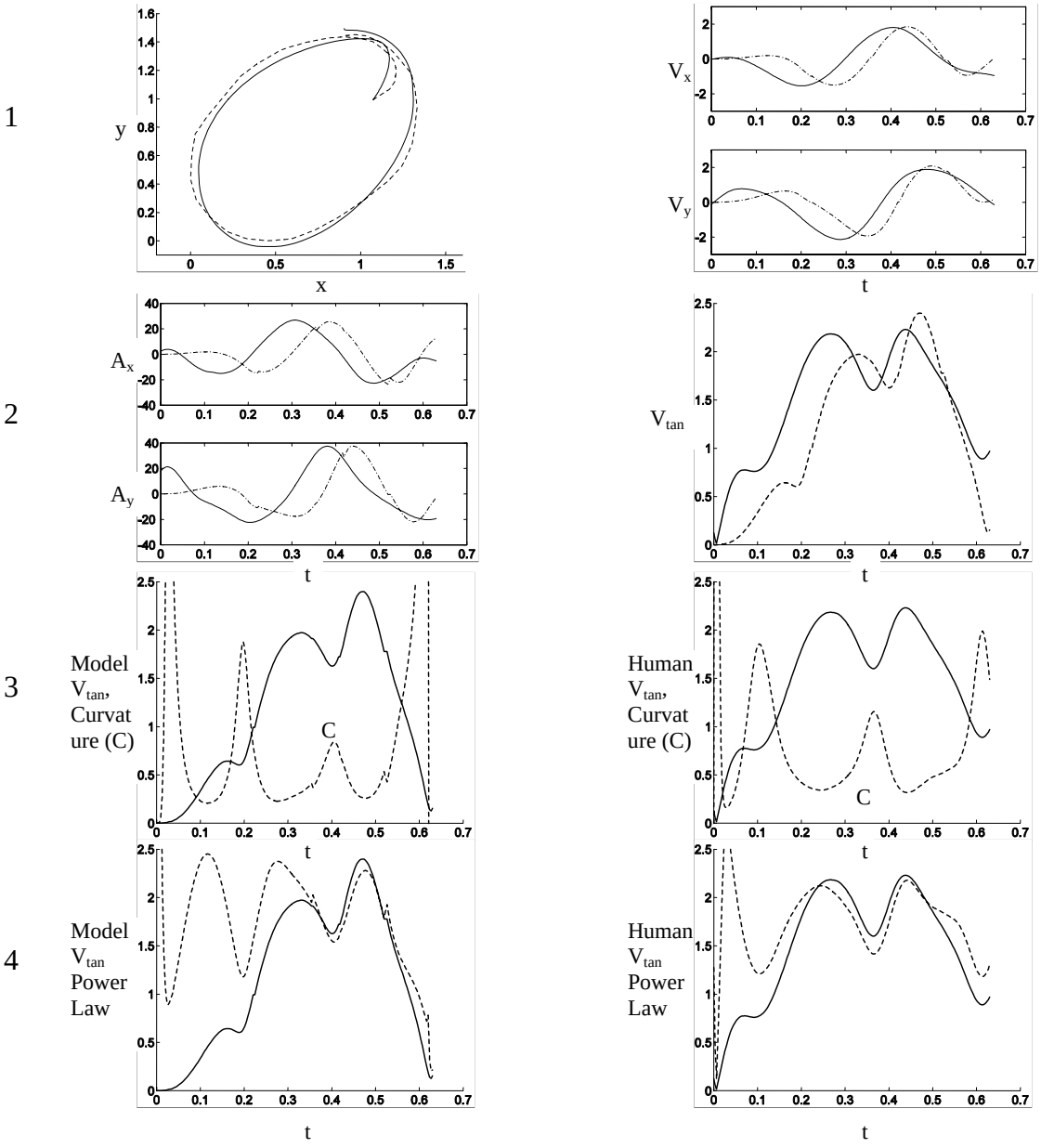

Fig. 4. Poor correlations for *O* subject 3. (1a) Human (dash) and model (solid) trajectory; (1b) Human (solid) and model (dash) velocity (x top); (2a) Human (solid) and model (dash) acceleration (x top); (2b) Human (solid) and model (dash) tangential velocity; (3a) Model tangential velocity (solid) and curvature (dash); (3b) Human tangential velocity (solid) and curvature (dash); (4a) Model 2/3 power law tangential velocity prediction (dash) vs. actual model tangential velocity (solid); (4b) Human 2/3 power law tangential velocity prediction (dash) vs. actual human tangential velocity (solid).

2b). The model's performance with non-zero starting velocities can be seen in comparing the second "e" to the first in the connected letters of Fig. 7. The average correlations between the tangential velocities predicted by the Two-Thirds Power Law and the model's and humans' tangential velocities are 0.83 +/- 0.10 (0.79 +/- 0.12, r = 0) for AVITEWRITE, and 0.86 +/- 0.07 (0.84 +/-0.09, r = 0) for the human data. Note that the 2/3 Power Law prediction of tangential velocity has singularities at points where the curvature is zero (Equations 15 and 17), which occurs at points of zero acceleration at the

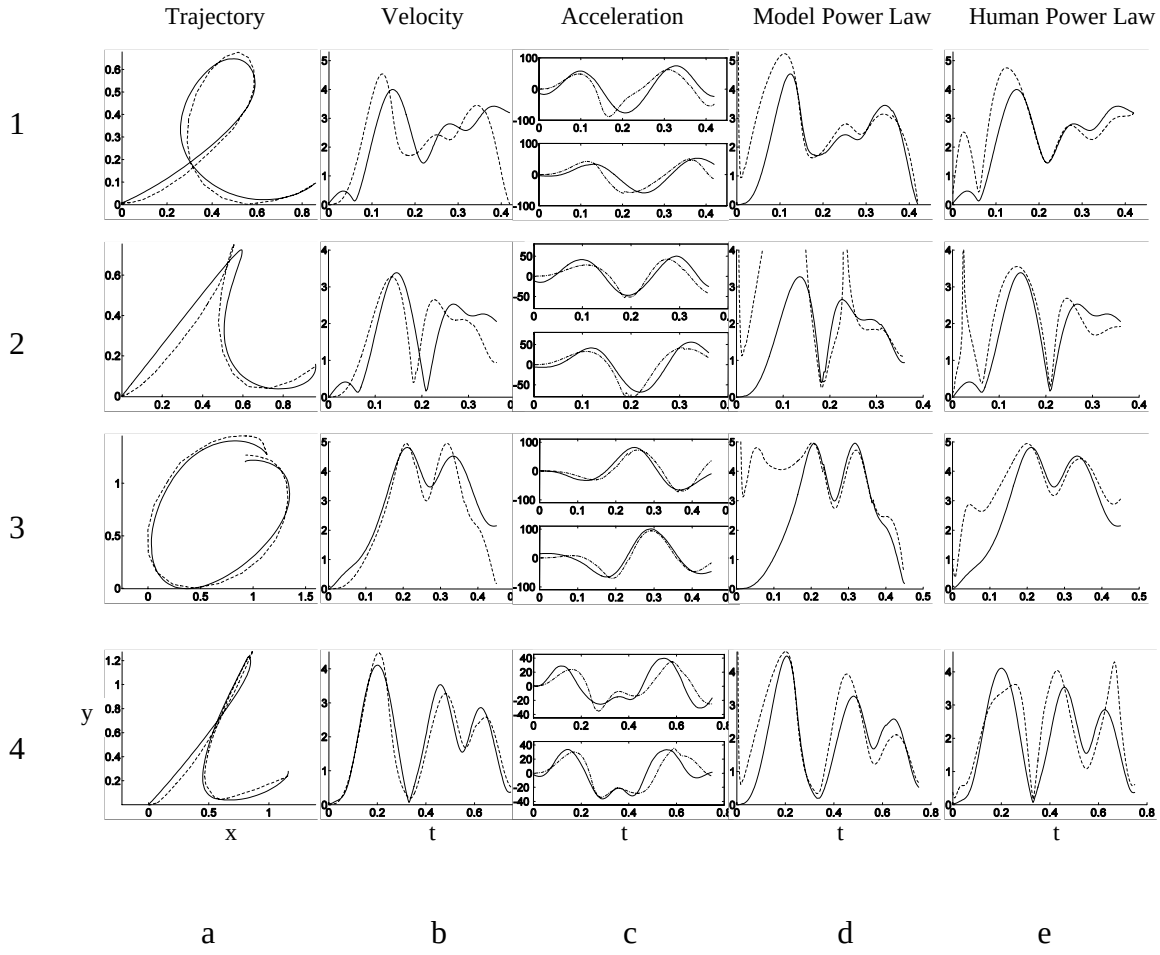

Fig. 5. Simulations with best correlations: (a) trajectory of model vs. human (dash); (b) tangential velocity of model (dash) vs. human (solid); (c) x (top) and y (bottom) acceleration of model (dash) vs. human (solid); (d) tangential velocity predicted by the 2/3 power law (dash) compared to model tangential velocity (solid); (e) tangential velocity predicted by the 2/3 power law (dash) compared to human tangential velocity (solid). (1) E of subject 1; (2) I of subject 1; (3) O of subject 7; (4) T of subject 4. See Table 2 for correlations.

start of each movement. These singularities were removed from the figures for clarity, and are the cause of the poor match between model output and 2/3 power law prediction at the extremes of the figures, as seen in Fig. 3 (4a). Note that a similar singularity occurs in the human data of Fig. 3 (4b).

Comparison of the averaged and unaveraged human data revealed slight differences, primarily in writing slant and size, with phase shifts in the kinematic profiles (Fig. 8). The mean correlation between the averaged and unaveraged letters of Subject 1 is 0.96 +/- 0.03. The model's correlations for the averaged and unaveraged letters of Subject 1 are 0.94 +/-0.09 and 0.87 +/-0.12, respectively. Given the high degree of similarity between the averaged and unaveraged human data, it is not surprising that model performance is comparable on both.

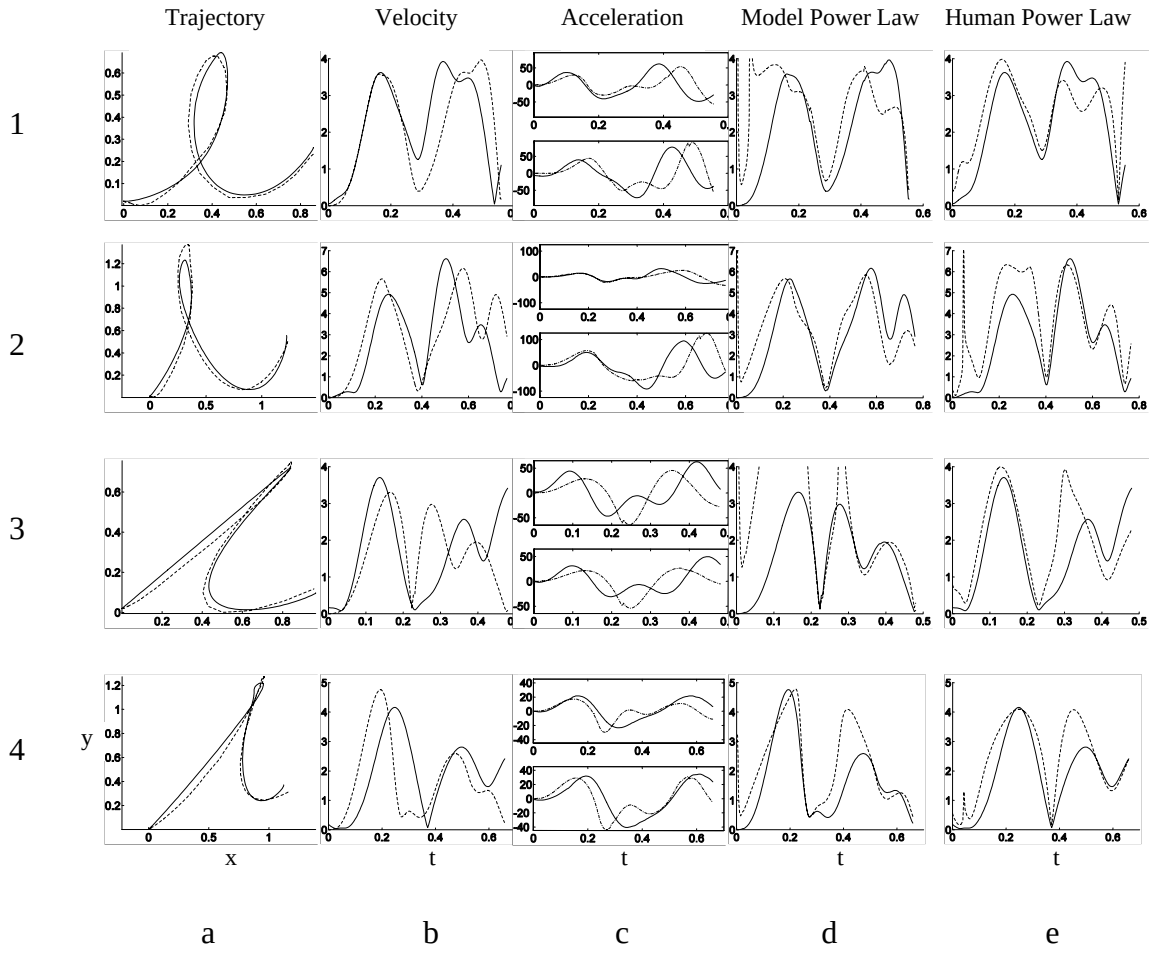

Fig. 6. Simulations with worst correlations: (a) trajectory of model vs. human (dash); (b) tangential velocity of model (dash) vs. human (solid); (c) x (top) and y (bottom) acceleration of model (dash) vs. human (solid); (d) tangential velocity predicted by the 2/3 power law (dash) compared to model tangential velocity (solid); (e) tangential velocity predicted by the 2/3 power law (dash) compared to human tangential velocity (solid). (1) E of subject 2; (2) L of subject 2; (3) I of subject 5; (4) T of subject 3. See Table 2 for correlations

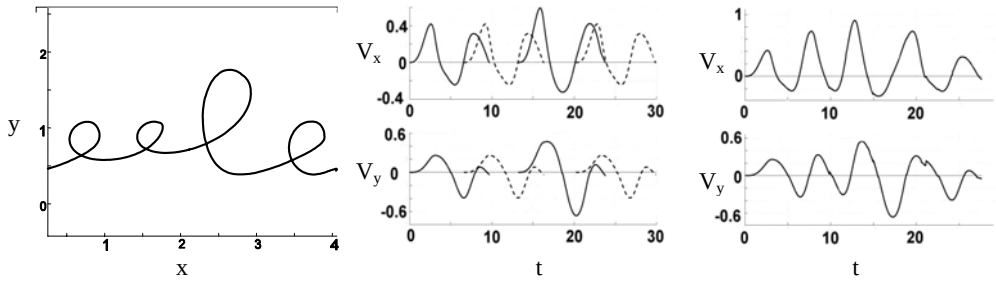

Fig. 7. Simulation of coarticulatory context effect by varying the overlap between adjacent letters. As seen also in human data from Thomassen & Schomaker (1986), the second *e* in *eele* is smallest due to overlap with the upstroke of the following *l*. (a) Model trajectory; (b) Individual velocity profiles of the letters staggered through time (x top, y bottom); (c) The velocity profile of the connected letters *eele* generated by AVITEWRITE. Reproduced with permission from Grossberg & Paine (2000).

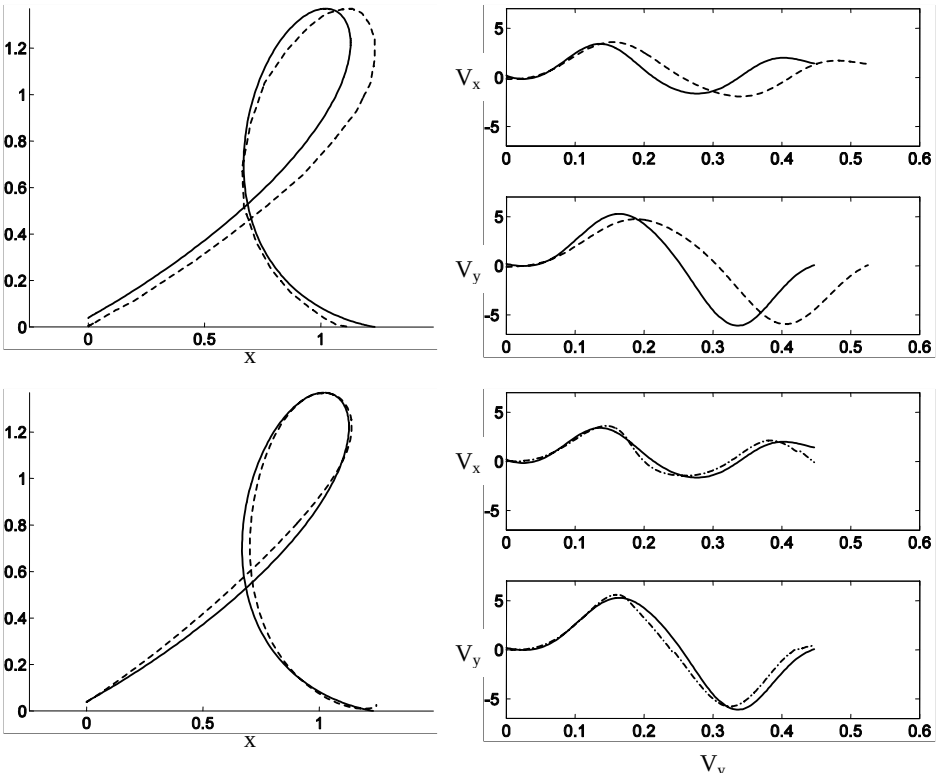

Fig. 8. Averaged versus Unaveraged data. Top Left: Trajectories of averaged (dash) and unaveraged (solid) letter L of Subject 1's trial 5. Top Right: Velocity (x top, y bottom) profiles of averaged (dash) and unaveraged (solid) data. Bottom Left: Trajectories of unaveraged (solid) and model (dash). Bottom Right: Velocity (x top, y bottom) profiles of unaveraged (solid) and model (dash).

IV. Discussion

This work further quantifies the performance of the AVITEWRITE handwriting learning model by comparing model performance to that of a group of human subjects. The model learned by tracing the trajectories for 5 average letters from 7 human subjects, for a total of 35 letters. Each average letter was generated from 10 writing samples per subject.

The only model parameter which was varied across letters and subjects was the attention radius, as seen in Appendix Table 4. AVITEWRITE makes essential use of visual spatial attention to determine where the hand will move to imitate a curve. Attention was modeled algorithmically since it was not the main focus of Grossberg and Paine (2000). The model assumes, for simplicity, that attention may be focused within a circular region around the present fixation point. In the model, visual spatial attention is initially focused around the current hand position on a template curve (Fig. 1, Box 1). If subsequent movement deviates from the attention radius around the curve due to memory inaccuracy, then a new target is chosen on the curve. Decreasing the attention radius increases the correlation between the model and the human subjects' performance (position, velocity, acceleration) at the cost of more learning trials for convergence to error-free performance. An excessively small attention radius may prevent convergence in a reasonable period of time, just as an excessively large attention radius will yield a poor trajectory, which converges quickly. The attention radius parameter value was manually tuned, so as to allow accurate trajectory generation with speedy convergence.

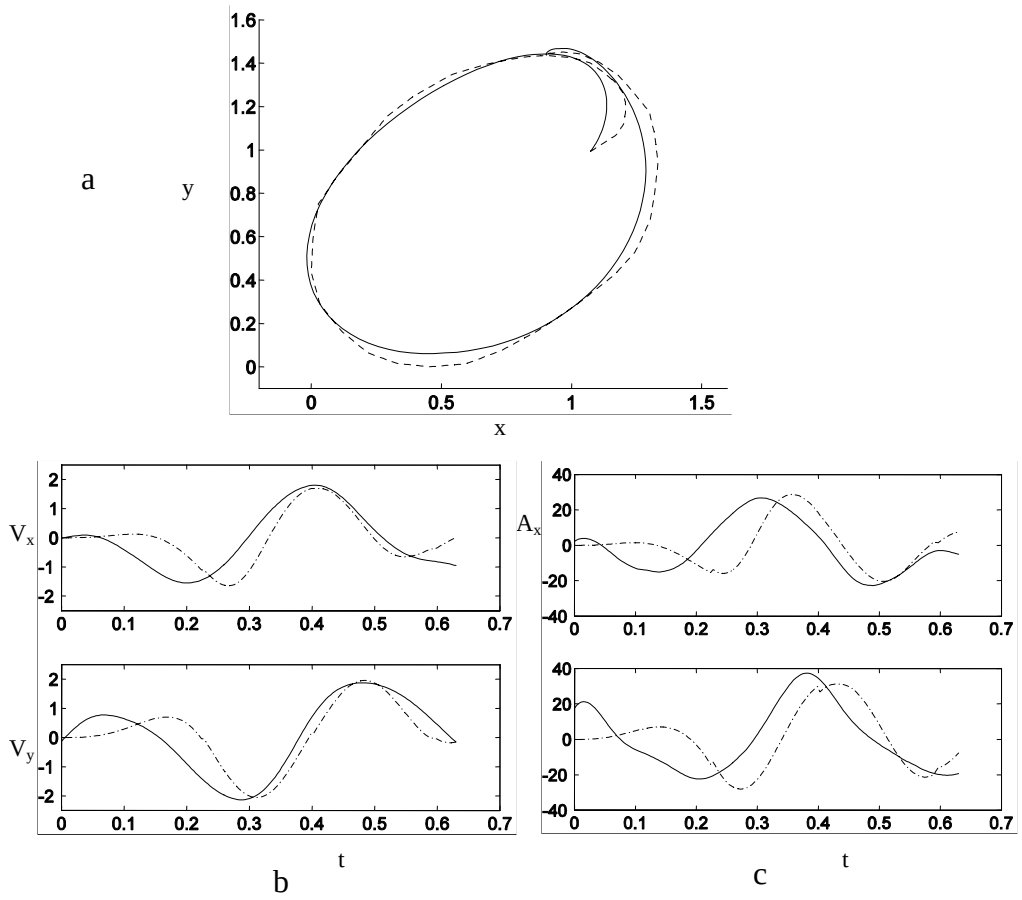

Fig. 9. Results of using a different spectral density (Δt = 0.055) and attention radius (r_a = 0.075) when AVITEWRITE learns the letter O from subject 3. (a) Trajectory of model (solid) and human (dash); (b) X(top) and Y (bottom) velocity of model (dash) and human (solid); (c) X (top) and Y (bottom) acceleration of model (dash) and human (solid). Compare with results when the same spectral density was used for all letters in Table 2 and Fig. 4.

Experimental data suggest that superior frontal, inferior parietal, and superior temporal cortex are part of a network for voluntary attention control (Hopfinger et al., 2000), which is critical for directing unpracticed movements (Richer et al., 1999, p. 1427). Jueptner et al. (1997a, 1997b) reported that the prefrontal cortex was activated in a finger movement-sequence learning task during new learning but not during automatic performance after learning. Further, the left dorsal prefrontal cortex was reactivated when subjects paid attention to the performance of a previously learned movement sequence (Jueptner et al., 1997b, p. 1313). Although no data are available that characterize a precise mechanism for modulating attention during movement learning, AVITEWRITE assumes that attention can be voluntarily controlled to achieve a desired level of accuracy, or else to complete learning in a limited time at the expense of accuracy.

Few published handwriting models attempt to measure their results through quantitative comparisons with a corpus of human data. One prior model, which is compared to a corpus of human data, is the Edelman and Flash (1987) minimum snap model. For this reason, we compare AVITEWRITE to the minimum snap model. A more

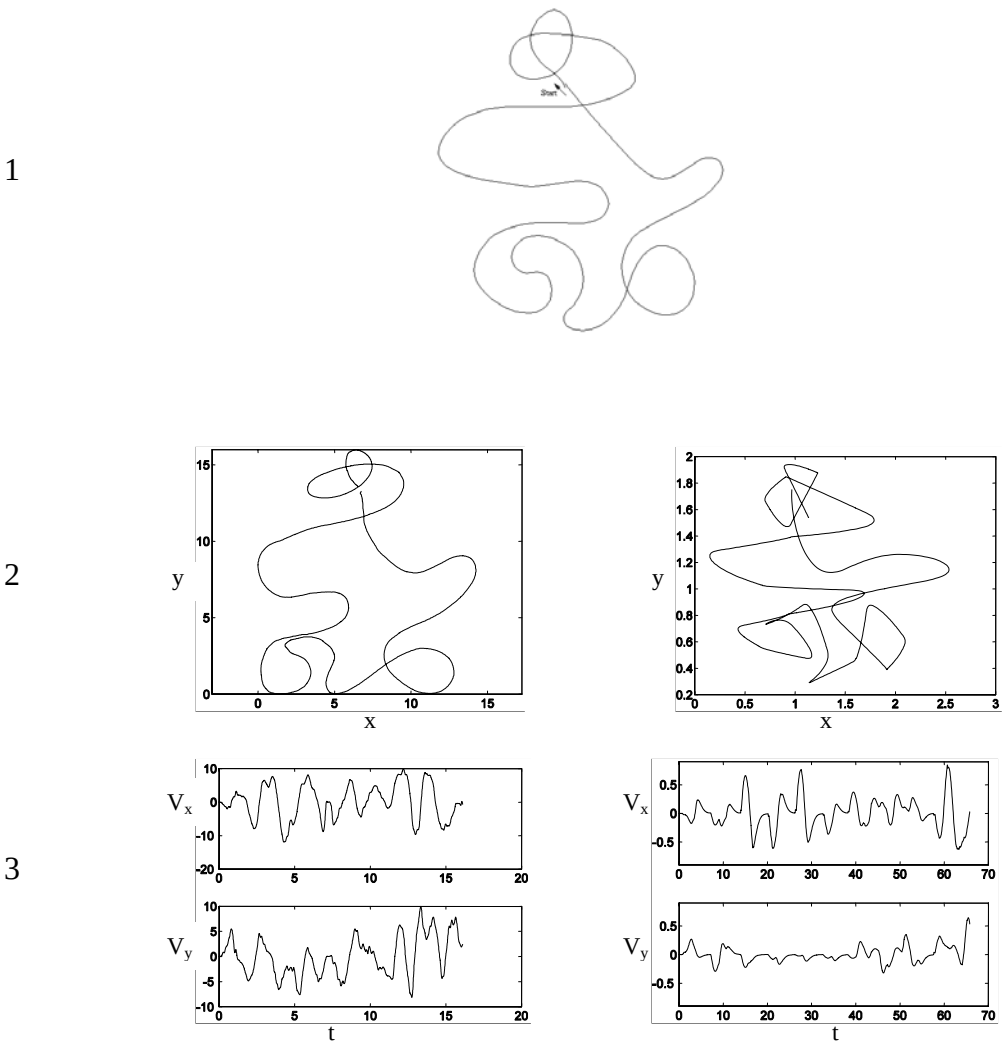

Fig. 10. Novel curve learning: (1) Template curve presented to human and model; (2a) Human trajectory on copying trial 1; (2b) AVITEWRITE model trajectory on tracing trial 1; (3a) Human x (top) and y (bottom) velocity profiles for the trajectory in 2a; (3b) AVITEWRITE x (top) and y (bottom) velocity profiles for the trajectory in 2b.

extensive review of handwriting models and discussion with regard to AVITEWRITE can be found in Grossberg and Paine (2000).

Edelman and Flash (1987) presented a bottom-up model of trajectory formation based on dynamic minimization of the square of the third (jerk) or fourth (snap) derivative of hand position. The version which minimizes snap yielded better correlation with human experimental data. The model assumes that all letters are formed by a concatenation of shape primitives, such as "cup", similar to a letter U, and "oval", like a letter O. Further, the model generates each stroke primitive by use of a via-point, an intermediate target prior to the end of the stroke. The model output is compared to human experimental data, and strong correlations are reported between model-generated position, velocity, and acceleration traces and the human counterparts. The inverse relation

between movement velocity and curvature seen in human writing is demonstrated by the model. The use of numerical estimations of the degree of fit to the data is emphasized and contrasted with the purely subjective fit estimates in some models.

One general problem with this hypothesis is that no known brain mechanisms can minimize a quantity across an entire movement trajectory before it occurs. Golgi tendon organs measure muscle tension (Gordon & Ghez, 1991). Further, Matthews (1972) showed that muscle receptors exist that are sensitive both to the length of the muscle and to the velocity of stretching. Thus, the first derivative of hand position is probably available to higher motor control centers. However, evidence supporting neural computation of higher derivatives of hand position is lacking. This raises the concern that jerk or snap minimization may be an epiphenomenon of human trajectory planning. Finally, the minimum snap model makes use of via-points, which are expressly chosen at the curvature maxima. In contrast, AVITEWRITE suggests an automatic, attention-based target selection algorithm.

Edelman and Flash (1987) computed the correlations of the minimum snap model to four curves (hook, cup, gamma, and oval) generated by three subjects, with ten curve samples per subject. Quantitatively, the minimum snap model yields better fits to the kinematic data than AVITEWRITE, with a mean correlation of 0.970, +/- 0.003, using cross-correlation with a variable permissible time shift (r) between data sequences (Table 1, Equation 14). However, it should be noted that the minimum snap model required the extraction of a different set of parameters from each curve in order to regenerate that curve. Such an approach tacitly assumes that a different subject generates each curve, which was not true in the experiments. The AVITEWRITE model also achieves higher correlations if parameters are varied in this way (e.g., an improvement from 0.63 to 0.76 as seen in Table 3 and Fig. 9). In the AVITEWRITE simulations that are reported here, only the attention radius was varied since varying levels of attention are known to affect task performance (Hopfinger et al., 2000; Richer et al., 1999; Jueptner et al., 1997a, 1997b). Other system parameters, such as those involved in the neuronal response dynamics and synaptic modification of Equations 1-3, were held constant based on the assumption that they would not vary significantly among different humans or different letters. The volitional speed command and the corresponding Purkinje cell spectral activation density (Δt) (Equations 2, 8, and 9) were held constant for this analysis, although Grossberg and Paine (2000) did show that improved performance may be achieved if learning begins at a slow speed and gradually increases across trials via increases in the volitional speed command (GO signal) and the spectral density. The "spectrum" refers to the phase-delayed pattern of Purkinje cell activation hypothesized to occur in response to a Conditioned Stimulus that arrives via parallel fibers at the Purkinje cell population. This pattern of Purkinje cell activity plays an important role in the hypothesized mechanism of adaptive timing used for movement learning in the AVITEWRITE model (Fiala, Grossberg, & Bullock, 1996; Grossberg & Merrill, 1992, 1996; Grossberg & Paine, 2000). The "spectral activation density" refers to the time delay between Purkinje cell activations. As seen in Fig. 4 (1a), the position correlation was relatively low (with a value of $c_x = 0.73$ and $c_y = 0.82$) for the letter "O" at the given GO signal and spectral density (Equations 2, 8, and 9) for the attention radius of 0.07, even though the same GO and spectral density yielded a much better result for the letter T for this same subject, with position $c_x = 0.94$ and $c_y = 1.0$ and an attention radius of 0.075.

Higher correlations could have been achieved if different parameters had been used. For example, a modest improvement in simulating subject 3's letter "O" can be achieved simply by increasing the spectral density and attention radius slightly, yielding a 0.13 improvement in overall correlation from 0.63 to 0.76 (Table 3, Fig. 9), with position c_x = 0.85 and c_y = 0.90. Seeking to test the model's applicability and generalizability to multiple letters and subjects, we focus on one parameter, attention, which turns out to have a strong, but not complete, influence on the intra- and inter-subject variability.

Parameters	X Position	Y Position	X Velocity	Y Velocity	X Acceler-ation	Y Acceler-ation	Average Correl-ation
$\Delta t = 0.06$ $r_a = 0.07$	0.73	0.82	0.68	0.76	0.37	0.43	0.63
$\Delta t = 0.055$ r_a=0.075	0.85	0.90	0.80	0.86	0.55	0.62	0.76

Table 3. Correlations between model performance and human data for Subject 3's letter O when spectral density (Δt) is varied as well as the attention radius (r_a).

This result points to one weakness of the current AVITEWRITE model, that is, the current lack of teaching signal normalization. For the letter "i" shown in Fig. 5 (2a), distant targets are initially chosen, yielding large Difference Vectors, due to the low curvature of the initial portion of the letter. (See Grossberg & Paine, 2000 for details of the target selection algorithm.) The initial, shallow curve of the "i" upstroke is approximated by AVITEWRITE as a nearly straight line for the attention radius of 0.07 used. As seen in Equations 3-7, the larger the Difference Vector, or DV, the larger the memory trace, and the resulting speed, other things being equal. Other things may not be equal, however, since the DV is gated by a volitional GO signal that releases the movement and controls overall movement speed (Bullock and Grossberg, 1988). Such a GO signal is controlled by the basal ganglia in the brain (Horak & Anderson, 1984a, 1984b; Turner et al., 1998). The present model simulations focus more on trajectory learning and performance by cortical and cerebellar circuits. For accurate learning and performance of letters of multiple sizes, the present simulations make clear that interactions of these brain regions with the basal ganglia are also needed. Related modeling work (e.g., Brown, Bullock, and Grossberg, 2002) has begun to clarify how these interactions work.

Further evaluation of the AVITEWRITE model would also be facilitated if there existed more studies of handwriting learning in children. Many handwriting studies have been done with children in order to improve the teaching of handwriting (Freeman, 1914; Burns, 1962; Hendricks, 1976; Furner, 1983). These studies reveal the progression of movement proficiency over years of practice. The fact that handwriting performance can improve over years of practice suggests that it is the result of cumulative learning from many individual writing trials. Unfortunately, few scientific studies of either adults or children address short-term changes in handwriting performance due to learning on individual movement trials. Preliminary attempts to learn a novel shape (Fig. 10) were begun as part of this work. However, only adult subjects were available for the experiments. These adults, with years of writing experience, were able to copy the novel

shape with smooth, continuous velocity profiles on the first trial, whereas AVITEWRITE begins learning each new shape in a naive state, and initially generates more segmented velocity profiles and straight line curve segments. These segmented velocity profiles reflect a more discrete, multiple-stroke-driven strategy on early movement trials in AVITEWRITE compared to adult humans (Fig. 10, see also Fig. 23 of Grossberg & Paine, 2000). Edelman and Flash (1987), among others (Morasso, 1986; Wing, 1980), propose that this problem may be overcome by learning a discrete set of motor primitives, which are then concatenated to generate arbitrary shapes. Although the AVITEWRITE model does not explicitly describe motor primitives, concatenation of learned letters with coarticulatory context effects (Fig. 7) was demonstrated in Grossberg and Paine (2000). The problem remains open of what motor primitives, including whole letter shapes, may be learned to generate a complex motor repertoire and how they may be rapidly assembled to generate an arbitrary, novel shape.

V. Conclusion

The AVITEWRITE model describes aspects of how the cerebral cortex, cerebellum, and basal ganglia may interact during complex learned handwriting movements. There is both cooperation and competition between reactive vision-based imitation and planned memory read-out. The model suggests that there is an automatic shift in the balance of movement control between cortical and cerebellar processes during the course of learning. AVITEWRITE shows how challenging psychophysical properties of planar hand movements may emerge from this cortico-cerebellar-basal ganglia interaction.

The present data from simulations using the AVITEWRITE model have highlighted some of its strengths while focusing attention on areas where all models of handwriting and the learning of other complex sensory-motor skills would benefit from further research. A key area concerns how to generalize prior sensory-motor learning to facilitate the learning of novel curves. Further evaluation of all handwriting models would also be facilitated by the availability of experiments that study novel curve learning in younger subjects, who may not yet have developed putative motor primitives or the skill for concatenating them for arbitrary novel curves.

Appendix

For a complete description of the model implementation, please see Grossberg and Paine (2000).

Model Equations

At the beginning of movement learning, a visual target position (*TPV*) is chosen in a predefined forward direction on the curve to be learned such that the line from the current hand position, *PPV*, to *TPV* never exceeds an attention threshold distance, or radius, from the curve being traced (the template curve). The difference vector to the target, DV_{vis}, is integrated toward the value of *TPV* - *PPV*, as in Equation (1):

Visual Difference Vector

$$\frac{dDV_{vis}}{dt} = [-\mu_1(DV_{vis}) + \mu_2(TPV - PPV)(1 - H(RH(tube) - \varepsilon))] \qquad (1)$$

In (1), *R* is the learned cerebellar output. *H(tube)* equals 1 if the *PPV* is within the attention radius of the template curve being traced, and it equals zero otherwise. $H(RH(tube) - \varepsilon)$ equals one if *PPV* is within the attention radius of the template curve and the cerebellar output, *R*, is above some threshold value, ε. $(1 - H(RH(tube) - \varepsilon))$ equals zero and the visual difference vector, DV_{vis}, decays to zero. In (1), $\mu_1 = 1$; $\mu_2 = 0.25$; and $\varepsilon = 0.001$. Thus, if memory is available and movement is sufficiently accurate, then memory directs the movement. If the memory signal is too small or an error is made by deviating from the attention radius around the template curve, then vision controls the movement direction.

Cerebellar learning is simulated as follows. A spectrum of Purkinje cell (PC) responses is created using Equation (2):

Cerebellar Spectral Component

$$g_i = \gamma((t - (i-1)\cdot\Delta t)^2)(B - (t - (i-1)\cdot\Delta t)^{2.9}). \qquad (2)$$

In (2), $\Delta t = 0.06$: The time between the start of adjacent Purkinje cell spectra. Term g_i models activation of Purkinje cell *i* at time *t*. $\gamma = 0.0136$ and $B = 25$.

The i^{th} synaptic weight z_i between the parallel fibers and the Purkinje cells is modified based on the climbing fiber inputs as described in Equation (3):

Cerebellar Synaptic Weights

$$\frac{dz_i}{dt} = \alpha_z g_i(-z_i + \alpha(TPV - PPV))\cdot H(TPV - PPV). \qquad (3)$$

Each synaptic weight is modified only if its spectral component g_i is active and visual target information is available. Visual target information is defined by *TPV*. Climbing fiber activity is assumed to be proportional to the size of the difference between the target position, *TPV*, and the present position, *PPV*, with synaptic weights increasing in proportion to the value of *TPV-PPV* in Equation (3). $H(TPV - PPV)$ equals 1 if $(TPV - PPV) > 0$, and it equals 0 otherwise. Parameters $\alpha_z = 0.3$ and $\alpha = 0.08$ in (3).

The gated spectral activity $h_i = g_i z_i$. Each term $g_i z_i$ provides a local view in time of the learned information. The sum of these terms provides a continuous sampling of the climbing fiber teaching signals. Thus, the population response of the Purkinje cells is summed to form the adaptively timed cerebellar output, *R*, as in Equation (4):

Adaptively Timed Cerebellar Output

$$R = \sum_i h_i \,. \tag{4}$$

The cerebellar output, *R*, is generated at a fixed rate in response to a given density of PC spectral components g_i through time. The output rate of *R* can be altered by changing spectral density. Decreasing spectral density allows movement learning at variable speeds.

A cortical Working Memory buffer is hypothesized to allow performance of learned movements at variable speeds while preserving movement and velocity profile shape. *R* is temporarily stored in a working memory buffer, simulated as a discretely sampled set of values from the continuous cerebellar output:

$$WM(t) = R(t_i) \text{ for } t_i < t < t_{i+1} \,. \tag{5}$$

In (5), t_i is the i^{th} time that DV_{gate}, which is defined in (11) below, becomes zero from a positive value. At time $t = 0$, $WM(0) = R(0)$. This working memory output, *WM*, is combined with the visual difference vector, DV_{vis}, and scaled by a size-controlling *GRO* signal, *S*, to form the size-scaled, memory-enhanced difference vector, DV_S:

$$DV_S = S \cdot (WM + DV_{vis}) \,. \tag{6}$$

In (6), $S = 0.3$

Present Position Vector

$$\frac{dPPV(t)}{dt} = DV_S \cdot GO(t) \,. \tag{7}$$

The speed-controlling *GO* signal is defined as follows:

***GO* Signal**

$$\frac{dG}{dt} = \gamma_1(-G + J) \tag{8}$$

$$GO = G(t) \,. \tag{9}$$

$J = 20$. Parameter $\gamma_1 = 8$.

Readout of the Working Memory buffer's discrete movement commands is controlled as follows. A memory-modulated target (TPV_m) is generated as follows:

Memory-Modulated Target

$$TPV_m(i+1) = TPV_m(i) + DV_S \,. \tag{10}$$

It tracks the cumulative DV_S through time. The *PPV* is subtracted from the TPV_m to form a

Gating Difference Vector

$$DV_{gate} = TPV_m - PPV \text{ .} \quad (11)$$

DV_{gate} controls readout from the WM buffer. The next cerebellar command that has been stored in Working Memory is read from the WM buffer when DV_{gate} is less than or equal to zero; that is, when the current TPV_m has been reached or surpassed. By altering the size of the *GO* signal, the rate at which TPV_m is reached by the outflow *PPV* can be controlled. Thus, Working Memory readout is controlled by the speed of the movement, which is determined by *PPV*. This gating rule ensures that the shapes of the movement and its velocity profile are preserved as performance speed is changed by a different choice of the volitional *GO* signal.

Letter	Average Attention Radius (r_a) +/- standard deviation	Average Number of Trials for Model to Learn +/- standard deviation
e	0.034 +/- 0.002	33 +/- 27
l	0.044 +/- 0.005	104 +/- 158 (range: 14-447)
i	0.054 +/- 0.010	20 +/- 24 (range: 4-74)
o	0.069 +/- 0.005	21 +/- 12
t	0.09 +/- 0.05	12 +/- 10

Table 4. Model parameters for five letters across seven subjects. Note: Attention radius (r_a) held constant during learning for a given subject's letter.

The movement velocity profiles generated by the model represent outflow movement commands, not the actual performance of the arm/hand system. There is filtering of the movement signal downstream of the central command by the peripheral muscle apparatus (Contreras-Vidal et al., 1997). An assumption of low-pass filtering in the command pathway is commonly made in muscle models (Barto et al., 1999, p.567). Therefore, the acceleration profile (12) generated by the present model is filtered using a first order differential equation (13):

Acceleration Profile

$$A(t) = \frac{\frac{dPPV(t)}{dt} - \frac{dPPV(t-D)}{dt}}{D} \quad (12)$$

Muscle-Filtered Acceleration Profile

$$\frac{dA_f}{dt} = (-A_f(t) + A(t)) \text{ .} \quad (13)$$

The step size in (12) is $D = 0.05$.

Correlation Equation (Edelman & Flash, 1987)

$$c(a,b) = \max_{0 \le r \le R} \frac{\sum_{i=0}^{n-r} (a_i - \bar{a})(b_{i+r} - \bar{b})}{(n-r)\sqrt{\frac{1}{n}\sum_{i=0}^{n} (a_i - \bar{a})^2} \cdot \sqrt{\frac{1}{n}\sum_{i=0}^{n} (b_i - \bar{b})^2}} \qquad (14)$$

Correlations were calculated for x and y position, velocity, acceleration, tangential velocity, and Two-Thirds Power Law tangential velocity predictions. Equation (14) defines the correlation for two sequences $a(t) = \{a_0, a_1, ..., a_n\}$ and $b(t) = \{b_0, b_1, ..., b_n\}$. $\bar{a}$ and $\bar{b}$ are the sequence means. R is the maximum permitted index shift between the two vectors and is equal to $0.1n$. Equation (14) is intended to yield correlations from -1 to 1, although values slightly greater than 1 can occur, as in Figs. 3 to 6 of Edelman and Flash (1987). Similar curves yield positive correlation values, although the curves are not necessarily identical.

Curvature

Observe the inverse relation between tangential velocity and curvature in Fig. 3 (3a, b). The peaks in curvature near the ends of the simulated trajectories (Fig. 3a) are the result of the x and y velocities (Vx, Vy) getting very small, with Vx and $Vy << 1$. As seen in Equation (15),

$$C = \frac{(Vx \cdot Ay) - (Vy \cdot Ax)}{(Vx^2 + Vy^2)^{1.5}} \qquad (15)$$

curvature C approaches infinity as the sum of Vx^2 and Vy^2 approaches zero.

Two-Thirds Power Law

The Two-Thirds Power Law states that the angular velocity is proportional to the curvature raised to the two-thirds power (Lacquaniti et al., 1983):

$$A = kC^{\frac{2}{3}}, \qquad (16)$$

where A = angular velocity, C = curvature, and k is a proportionality constant. Equivalently,

$$V_{\tan} = kr^{\frac{1}{3}}, \qquad (17)$$

where V_{tan} = tangential velocity, r = radius of curvature ($1/C$), and k is a proportionality constant.

References

Abend, W., Bizzi, E., Morasso, P. (1982). Human arm trajectory formation. *Brain*, **105**, 331-348.

Alston, J., Taylor, J. (1987). *Handwriting: Theory, Research, and Practice*. New York: Nichols.

Andersen, R. (1995). Encoding of intention and spatial location in the posterior parietal cortex. *Cerebral Cortex*, **5**, 457-469.

Barto, A. G., Fagg, A. H., Sitkoff, N., Houk, J. C. (1999). A cerebellar model of timing and prediction in the control of reaching. *Neural Computation*, **11**, 565-594.

Brown, J.W., Bullock, D., and Grossberg, S. (2002). How laminar frontal cortex and basal ganglia circuits interact to control planned and reactive saccades. CAS/CNS Technical Report 2000-023. Submitted for publication.

Bullock, D., Cisek, P., Grossberg, S. (1998). Cortical Networks for Control of Voluntary Arm Movements Under Variable Force Conditions. *Cerebral Cortex*, **8**, 48-62.

Bullock, D. and Grossberg, S. (1988). Neural dynamics of planned arm movements: Emergent invariants and speed-accuracy properties during trajectory formation. *Psychological Review*, **95**, 49-90.

Burns, P.C. (1962). *Improving Handwriting Instruction in Elementary Schools Minneapolis*, (pp.45-46). Minneapolis, MN: Burgess Publishing Co.

Contreras-Vidal J.L., Grossberg, S., Bullock, D. (1997). A neural model of cerebellar learning for arm movement control: Cortico-Spino-Cerebellar dynamics. *Learning and Memory*, **3**, 475-502.

Edelman, S., Flash, T. (1987). A model of handwriting. *Biological Cybernetics*, **57**, 25-36.

Fiala, J., Grossberg, S., Bullock, D. (1996). Metabotropic glutamate receptor activation in cerebellar Purkinje cells as substrate for adaptive timing of the classically conditioned eye-blink response. *The Journal of Neuroscience*, **16**, 3760-3774.

Freeman, F. N. (1914). *The Teaching of Handwriting*, (pp. 83-84). Boston, MA: Houghton-Mifflin, The Riverside Press Cambridge.

Furner, B. (1983). Developing handwriting ability: A perceptual learning process. *Topics in Learning and Learning Disabilities*, **3**, 41-54.

Georgopoulos, A. P., Kalaska, J. F., Caminiti, R., Massey, J. T. (1982). On the relations between the direction of two-dimensional arm movements and cell discharge in primate motor cortex. *Journal of Neuroscience*, **2**, 1527-1537.

Gordon, J., Ghez, C. (1991). Muscle receptors and spinal reflexes: The stretch reflex. In E.R. Kandel, J.H. Schwartz, T.M. Jessel (Eds.). *Principles of Neural Science*, pp. 564-580. New York: Elsevier Science Publishers.

Greer, K., Green, D. (1983). Context and motor control in handwriting. *Acta Psychologica*, **54**, 205-215.

Grossberg, S., Merrill, J. (1992). A neural network model of adaptively timed reinforcement learning and hippocampal dynamics. *Cognitive Brain Research*, **1**, 3-38.

Grossberg, S., Merrill, J. (1996). The hippocampus and cerebellum in adaptively timed learning, recognition, and movement. *Journal of Cognitive Neuroscience*, **8**, 257-277.

Grossberg, S., Paine, R. W. (2000). A neural model of corticocerebellar interactions during attentive imitation and predictive learning of sequential handwriting movements. *Neural Networks*, **13**(8-9), 999-1046.

Hendricks, W. (1976). *SCRIBE: Suggested Activities to Motivate the Teaching of Elementary Handwriting.* (p. 113). Stevensville, Michigan: Educational Service.

Hertrich, I., Ackermann, H. (1995). Coarticulation in slow speech: durational and spectral analysis. *Language and Speech*, **38**, 159-187.

Hopfinger, J. B., Buonocore, M. H., Mangun, G. R. (2000). The neural mechanisms of top-down attentional control. *Nature Neuroscience*, **3**, 284-291.

Horak, F. B., Anderson, M. E. (1984a). Influence of globus pallidus on arm movements in monkeys, I. Effects of kainic acid-induced lesions. *Journal of Neurophysiology*, **52**, 290-304.

Horak, F. B., Anderson, M. E. (1984b). Influence of globus pallidus on arm movements in monkeys, II. Effects of stimulation. *Journal of Neurophysiology*, **52**, 305-322.

Ito, M. (1984). *The Cerebellum and Neural Control*, (pp. 325-349). New York: Raven.

Jueptner, M., Frith, C. D., Brooks, D. J., Frackowiak, R. S., Passingham, R. E. (1997a). Anatomy of motor learning. II. Subcortical structures and learning by trial and error. *Journal of Neurophysiology*, **77**, 1325-1337.

Jueptner, M., Stephan, K. M., Frith, C. D., Brooks, D. J., Frackowiak, R. S., Passingham, R. E. (1997b). Anatomy of motor learning. I. Frontal cortex and attention to action. *Journal of Neurophysiology*, **77**, 1313-1324.

Lacquaniti, F., Terzuolo, C., Viviani, P. (1983). The law relating the kinematic and figural aspects of drawing movements. *Acta Psychologica*, **54**, 115-130.

Matthews, P.B.C. (1972). *Mammalian muscle receptors and their central actions*. Baltimore, MD: Williams and Wilkins.

Morasso, P. (1981). Spatial control of arm movements. *Experimental Brain Research*, **42**, 223-227.

Morasso, P. (1986). Understanding cursive script as a trajectory formation paradigm. In H. Kao, G. van Galen, R. Hoosain (Eds.). *Graphonomics: Contemporary Research in Handwriting*, pp. 137-167. New York: Elsevier Science Publishers.

Morasso, P., Mussa Ivaldi, F. A., Ruggiero, C. (1983). How a discontinuous mechanism can produce continuous patterns in trajectory formation and handwriting. *Acta Psychologica*, **54**, 83-98.

Mussa-Ivaldi, F. (1988). Do neurons in the motor cortex encode movement direction? An alternative hypothesis. *Neuroscience Letters*, **91**, 106-111.

Ostry, D., Gribble, P., Gracco, V. (1996). Coarticulation of jaw movements in speech production: is context sensitivity in speech kinematics centrally planned? *The Journal of Neuroscience* **16**, 1570-1579.

Perrett, S.P., Ruiz, B.P., Mauk, M.D. (1993). Cerebellar cortex lesions disrupt learning-dependent timing of conditioned eyelid responses. *The Journal of Neuroscience*, **13**, 1708-1718.

Plamondon, R., Alimi, A. (1997). Speed/accuracy trade-offs in target-directed movements. *Behavioral and Brain Sciences*, **20**, 279-349.

Richer, F., Chouinard, M. J., Rouleau, I. (1999). Frontal lesions impair the attentional control of movements during motor learning. *Neuropsychologia*, **37**, 1427-1435.

Schillings, J., Meulenbroek, R., Thomassen, A. (1996). Limb segment recruitment as a function of movement direction, amplitude, and speed. *Journal of Motor Behavior*, **28**, 241-254.

Teulings, H.L., Maarse, F.J. (1984). Digital recording and processing of handwriting movements. *Human Movement Science*, **3**, 193-217.

Teulings, H.L., Stelmach, G.E. (1991). Control of stroke size, peak acceleration, and stroke duration in Parkinsonian handwriting. *Journal of Movement Sciences*, **10**, 315-333.

Thomassen, A., Schomaker, L. (1986). Between-letter context effects in handwriting trajectories. In H. Kao, G. van Galen, R. Hoosain (Eds.). *Graphonomics: Contemporary Research in Handwriting*, pp. 253-272. New York: North-Holland: Elsevier Science Publishers.

Thomassen, A., Teulings, H. (1985). Time, size and shape in handwriting: exploring spatio-temporal relationships at different levels. In J. Michon, J. Jackson, (Eds.). *Time, Mind, and Behavior*, pp. 253-263. Berlin: Springer-Verlag.

Turner, R. S., Grafton, S. T., Votaw, J. R., Delong, M. R., Hoffman, J. M. (1998). Motor subcircuits mediating the control of movement velocity: A PET study. *Journal of Neurophysiology*, **80**, 2162-2176.

Van Galen, G.P., Weber, J. (1998). On-line size control in handwriting demonstrates the continuous nature of motor programs. *Acta Psychologica*, **100**, 195-216.

Van Gemmert, A. W. A., Adler, C. H., Stelmach, G. E. (2003). Parkinson's disease patients undershoot target size in handwriting and similar tasks. *Journal of Neurology, Neurosurgery, and Psychiatry*, **74**, 1502-1508.

Wann, J., Nimmo-Smith, I., Wing, A. (1988). Relation between velocity and curvature in movement: equivalence and divergence between a power law and a minimum-jerk model. *Journal of Experimental Psychology: Human Perception and Performance*, **14**, 622-637.

Wann, J. P., Nimmo-Smith, I. (1990). Evidence against the relative invariance of timing in handwriting. *The Quarterly Journal of Experimental Psychology*, **42A**, 105-119.

Wing, A. M. (1980). Response timing in handwriting. In: Stelmach, G. E. (Ed.). *Information Processing in Motor Control and Learning*, pp. 153-172. New York: Academic Press.

Wright, C.E. (1993). Evaluating the special role of time in the control of handwriting. *Acta Psychologica*, **82**, 5-52.